SPANDIDOS PUBLICATIONS EXPERIMENTAL AND THERAPEUTIC MEDICINE 19: 3675-3683, 2020

Differential diagnosis of thyroid nodules through a combination of multiple ultrasonography techniques: A decision-tree model

WEN LUO[1*], YUNFEI ZHANG[2*], JIANI YUAN[1*], XIAO YANG[1], LINA PANG[1], LEI DING[1], PEIDI ZHANG[1], LIWEN LIU[1] and XIAODONG ZHOU[1]

[1]Department of Ultrasound, Xijing Hospital, Fourth Military Medical University, Xi'an, Shaanxi 710032; [2]Research Institution of Bone Tumor, Tangdu Hospital, Fourth Military Medical University, Xi'an, Shaanxi 710038, P.R. China

Received March 21, 2019; Accepted December 18, 2019

DOI: 10.3892/etm.2020.8621

Abstract. The present study aimed to establish a decision tree (DT) model by combining the parameters of conventional gray-scale ultrasonography (US), elastosonography (ES), color Doppler US (CDUS) and contrast-enhanced US (CEUS) for the differential diagnosis of thyroid nodules. A single-center, retrospective study of 321 thyroid nodules was conducted. For 222 nodules, parameters of conventional gray-scale US, CDUS, ES and CEUS were evaluated using univariate logistic regression. Factors for with P<0.10 were further assessed using multivariate logistic regression. Significant factors (P<0.05) were used to establish a DT. The diagnostic accuracy of this DT was then evaluated by its application to the other 99 nodules. After univariate logistic analysis, factors including gender, number of nodules and diffuse disease were excluded, due to P>0.10. The results of multivariate logistic analysis determined that the following factors were required for the DT: Extent of blood flow determined by CDUS (P=0.002), area ratio determined by ES (P=0.033), peak phase patterns determined by CEUS (P<0.001) and micro-calcification determined by conventional gray-scale US (P=0.015). When compared to the pathological or cytological results of 99 nodules, the resulting DT had a sensitivity of 98.6%, specificity of 80.1%, positive predictive value of 93.5% and negative predictive value of 95.5%. These results suggested that a DT combining conventional gray-scale US, ES, CDUS and CEUS may be helpful for differentiating between types of thyroid nodules.

Correspondence to: Dr Liwen Liu or Dr Xiaodong Zhou, Department of Ultrasound, Xijing Hospital, Fourth Military Medical University, 127 Changle Xi Road, Xi'an, Shaanxi 710032, P.R. China
E-mail: liuliwen@fmmu.edu.cn
E-mail: zxdlwdd@163.com

*Contributed equally

Key words: thyroid nodules, ultrasonography, elastosonography, contrast-enhanced sonography, decision tree

Introduction

Due to the rapid development of medical imaging technology, the clinical detection of thyroid nodules has increased worldwide, allowing for higher rates of thyroid cancer diagnosis (1-3). Acar *et al* (4) reported 51% of patients who had been referred to their radiology department undergoing high-resolution ultrasonography (US) were found to have at least one thyroid nodule. Managing these thyroid nodules, making a treatment plan and predicting patient prognosis all require the clinician to accurately distinguish malignant from benign nodules, which remains a challenge for both doctors and sonographers (5). Medical imaging is critical to the diagnosis of thyroid nodules. However, the limited resolution of cross-sections from computed tomography, magnetic resonance imaging and positron emission tomography provide little useful information for the diagnosis of small nodules (6-8). Technological advances, including higher resolution and reproducibility, and the advantages associated with the lack of radiation, have pushed US imaging toward the frontline of differential diagnosis. The use of high-resolution US could remove the need for excessive fine needle aspiration (FNA) and also supply information for the design of appropriate surgical programs for cases of undetermined cytology (9).

In the past several years, the US-based diagnosis of thyroid nodules has relied primarily upon conventional gray-scale US. Using this method, malignancy was shown to be associated with hypoechogenicity, height greater than length, blur margin and micro-calcification (10,11). However, small nodules, which make up the majority of observed nodules, appear with more atypical features on conventional gray-scale US. Fortunately, new US techniques have been developed and clinically applied. For example, contrast-enhanced US (CEUS) employs a microbubble agent to enhance the backscatter signals of red blood cells and can be used to characterize local vascular perfusion. Several studies have explored the perfusion patterns of thyroid nodules using CEUS (12-14). Elastosonography (ES) can be used to estimate malignancy by assessing the hardness of tissues (15). Although the diagnostic accuracy of ES alone is not optimal, the information it supplies is useful when combined with that obtained via other US techniques (16). These advanced integrative techniques reportedly improved the diagnostic accuracy of the thyroid image reporting and data

system (TI-RADS) (17). However, to the best of our knowledge, no previous study has provided a systematic method for integrating US parameters from multiple techniques; physicians and sonographers are sometimes overwhelmed by the large amount of information acquired (18).

In the present preliminary study, to establish an efficient strategy for differential diagnosis of thyroid nodules using a combination of US techniques, multiple features presented by conventional gray-scale US, color Doppler US (CDUS), ES and CEUS were assessed using univariate and multivariate logistic regression. The significant factors obtained were then integrated using a decision tree (DT) model.

Materials and methods

Patients. The current study was approved by The Ethics Committee of the First Affiliated Hospital of the Fourth Military Medical University and approval for using the medical records of the patients was acquired. Patients who had undergone thyroid US examination in the department of ultrasound in Xijing Hospital during the period between January 2014 and January 2016 were enrolled retrospectively, according to the following criteria: i) The diagnosis of nodules was confirmed using pathological results after surgery or cytological evidence after FNA; and ii) these nodules were scanned using 2D gray-scale US, CDUS, CEUS and ES. The scanning sequence of 2D gray-scale US, CDUS, CEUS and ES had no influence on results. The images from the patients were retrospectively reviewed for analysis.

Patients were excluded if no pathological or cytological results had been acquired, or if a US scan was not available due to patient refusal or inappropriate physiological conditions, such as nodules that were too large to be measured on ES or unsuppressed swallowing action.

The final cohort included 296 patients with 321 nodules, the final diagnosis of which was confirmed by pathology after surgery (n=289) and cytology after FNA (n=32; Table I). Taking into consideration the pathological, cytological and laboratory results, 24 of the 321 nodules in this study were confirmed as inflammatory nodules caused by Hashimoto's thyroiditis, subacute thyroiditis or granuloma. Of 321 nodules, 222 (74 benign and 148 malignant) were used to build the DT model. The other 99 nodules (27 benign and 72 malignant) were used to assess the diagnostic accuracy of the DT model.

The excluded cases included 10 nodules that could not be measured using ES because of maximum diameters >3.5 cm, three nodules that yielded unsatisfactory ES images because of their isthmus location, and four nodules with unsuccessful CEUS cineloops owing to unsuppressed swallowing behavior.

Equipment and US examination. The patients were positioned in a supine position with their necks hyperextended to expose the anterior cervical region. The Mylab™ 90 (Esaote SpA) ultrasound image system was used for US examination, the L522 probe (4-9 MHz; Esaote SpA) for CEUS and the L523 probe (7.5-13.0 MHz, Esaote SpA) for conventional gray-scale US, CDUS and ES. Conventional gray-scale US was performed to count, localize and characterize nodules. The CDUS scale was set at 5 cm/sec. Real-time ES was completed manually using a vibrating transducer (Esaote SpA). The rectangular region of interest was set to include the nodule as well as surrounding areas. The degree of tissue hardness was indicated by a color scale, wherein blue represented hard and red soft. Images from conventional gray-scale US, CDUS and ES were stored for later use.

For CEUS, the contrast agent SonoVue® (Bracco Imaging SpA) was administered through a forearm vein in a bolus of 1 ml followed by 5 ml of 0.9% saline. The cineloops from 0-90 sec after agent administration were stored. If multiple lesions existed, only one or two suspicious or representative nodules were scanned, because microbubbles emerge in thyroid tissue for only seconds and because the injection times were limited. One sonographer with 10 years of experience in US examination, who was blinded to all patient data, performed all four techniques.

Image analysis. The four categories of images (conventional gray-scale US, ES, CDUS and CEUS) were reviewed offline by two sonographers, each with 15 years of experience in US examination. The analysis of each category was separated by 2 weeks to avoid recall bias. The reviewers were blinded to clinical history, the results of other examinations and pathology. Any disagreement between reviewers was settled by consultation with a third sonographer.

The parameters of the four imaging techniques are shown in Table II. The CEUS procedure occurred in three phases: The early phase, comprising the initial microbubble appearance to ~2 sec later; the peak phase, at the time-point when the enhancement intensity of nodules reached its maximum; and the late phase, from ~5 sec after the peak phase to the end of the recording. Each phase exhibited unique enhancement patterns. Pattern I was characterized by heterogeneous hypoenhancement (echogenicity less than that of surrounding thyroid tissue; Fig. 1A), Pattern II by homogeneous isoenhancement (echogenicity equal to that of surrounding thyroid tissue; Fig. 1B) and Pattern III by homogeneous enhancement with ring-like surrounding vascularity (Fig. 1C), mixed island-like enhancement (Fig. 1D) or no perfusion (Fig. 1E). Mixed island-like enhancement describes conditions in which perfusion within the nodules contains an anechoic portion (also termed a 'lake') and a portion with echogenicity equal to that of the surrounding thyroid tissue (also termed an 'island'; Fig. 1D); these two areas are clearly demarcated.

On conventional gray-scale US, echogenicity was categorized as follows: Pattern A, hyperechogenecity higher than or isoechogenecity equal to that of the surrounding thyroid tissue, or mixed with an echogenecity; Pattern B, hypoechogenicity, similar to that of the sternocleidomastoid (SCM); and Pattern C, hypoechogenicity lower than that of the SCM. Additional nodule parameters investigated included shape, margin, halo ring (hypoechoic area surrounding the nodules), micro-calcification and ratio of anteroposterior to transverse dimension (A/T ratio; Fig. 2). Diffuse change (the heterogeneous echogenicity of surrounding thyroid tissue) was also evaluated. On ES, the area ratio was calculated as the area of blue (high tissue hardness) within the nodule divided by the area of the entire nodule (Fig. 3A). Areas were manually traced by two sonographers using US equipment. After tracing, the area ratio was calculated automatically on-site. To calculate

Table I. Final diagnosis of nodules.

Final diagnosis	Total no. of nodules	Pathological category	No. of nodules
Histological results after surgery	289	Follicular carcinomas	5
		Medullary carcinoma	1
		Papillary carcinomas	204
		Nodular goiter	51
		Adenoma	5
		Inflammatory changes (Hashimoto's thyroiditis, subacute thyroiditis or granuloma)	23
Cytological results after FNA	32	Benign follicular epithelial cells	31
		Papillary carcinomas	1

FNA, fine-needle aspiration.

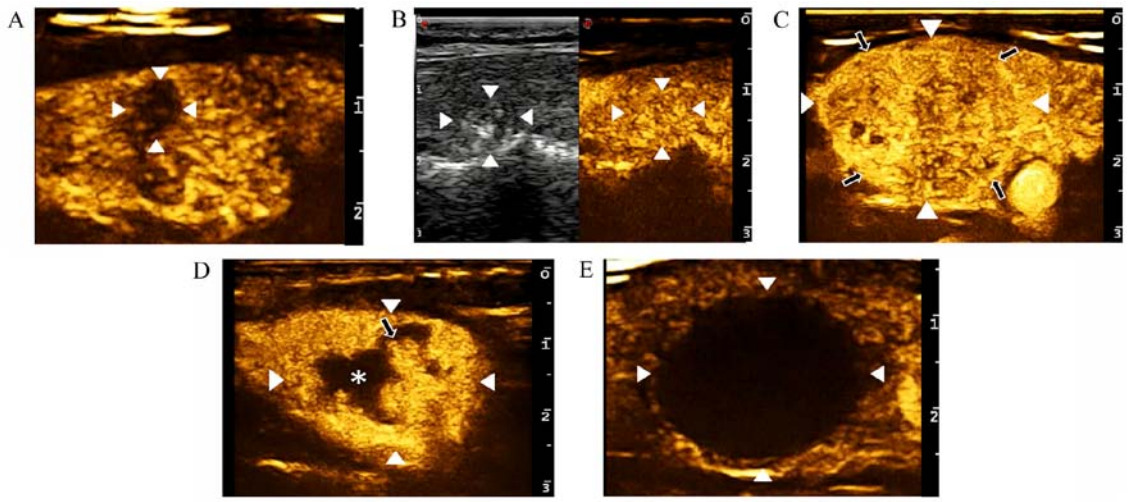

Figure 1. Peak-phase patterns of nodules obtained using contrast-enhanced ultrasonography. (A) Heterogeneous hypoenhancement (Pattern I) in a thyroid nodule of a 45-year-old woman. (B) Homogenous isoenhancement (Pattern II) in a thyroid nodule of a 38-year-old woman. (C) Homogenous isoenhancement with ring-like vascularity (Pattern III) in a thyroid nodule of a 42-year-old man (arrows indicate ring-like vascularity). (D) Mixed-island perfusion (Pattern III) in a thyroid nodule of a 50 year-old man (the black arrow indicates a parenchymal part of the nodule, the star indicates the cystic part of the nodule). (E) No perfusion (Pattern III) in a thyroid nodule of a 20-year-old woman. White arrowheads indicate nodules.

the elasticity index, an elliptical region of interest was manually adjusted in size so that it contained the entire nodule. The elasticity index was calculated as nodule elasticity divided by the elasticity of surrounding areas at similar depth (Fig. 3B). Each nodule was traced five times by each sonographer. The average result was recorded.

On CDUS, the extent of blood flow was defined as either low (minimal 'dot-like' blood flow detected), moderate (area of vascularity occupied about half the nodule), or high (area of vascularity covered more than half the nodule; Fig. 4). The presence of central vessels within nodules as well as 'ring-like' vascularity surrounding nodules was additionally reviewed.

Statistical analysis. All statistical analyses were performed using SPSS 13.0 (SPSS, Inc.) software. Descriptive analysis was performed using an independent sample t-test for continuous variables and the χ^2 test for categorical variables. Univariate logistic analysis was used to select the parameters with significance ($P<0.10$). Multivariate logistic analysis was then used to identify factors with the strongest association ($P<0.05$). Finally, exhaustive χ^2 Automatic Interaction Detection analysis was used to develop the DT using the data of the 222 nodules collected between January 2014 and April 2015. In the current study, any nodes with <10 subjects were considered as the final stop; there were at least five subjects in each leaf.

For elasticity index and area ratio on ES, the receiver operating characteristic (ROC) curve was used to determine the cutoff point, which was employed to change continuous variables to categorical variables when the DT model was set.

Characteristics of the DT, including sensitivity, specificity, positive predictive value, negative predictive value and their 95% confidence intervals (CI), were calculated using the data of the 99 nodules collected between May 2015 and January 2016.

The statistical analysis of the present manuscript included two parts, the first was to establish a DT algorithm using the data of 222 nodules; the second was to verify the diagnostic accuracy of the DT algorithm by using the data of 99 nodules.

Table II. Categories and parameters assessed on 2D gray-scale US, CD US, elastosonography and CE US.

A, Demographic data

Parameter	Benign (n=74)	Malignant (n=148)	P-value
Sex			0.646[a]
Male	16	38	
Female	58	110	
Age	45.9±11.3	43.5±11.5	0.136[b]
Nodule number			0.886[b]
Multiple	43	83	
Single	31	65	
Diameter mm	1.98±1.14	0.87±0.46	<0.001[b]

B, CE US

Parameter	Benign (n=74)	Malignant (n=148)	P-value
Early phase			<0.001[a]
Pattern I	11	120	
Pattern II	22	27	
Pattern III	41	1	
Peak phase			<0.001[a]
Pattern I	10	114	
Pattern II	12	33	
Pattern III	52	1	
Late phase			<0.001[a]
Pattern I	19	107	
Pattern II	27	35	
Pattern III	28	6	

C, Conventional gray-scale US

Echogenecity			<0.001[a]
Pattern A: Hyper-/iso-echogenecity; or mixed with anechogenecity	39	3	
Pattern B: Hypoechogenicity similar to that of SCM	9	22	
Pattern C: Echogenicity lower than that of SCM	26	123	
Halo ring			<0.001[a]
Yes	34	9	
No	40	139	
Margin			<0.001[a]
Clear	50	32	
Unclear	24	116	
Shape			<0.001[a]
Regular	50	17	
Irregular	24	131	
A/T ratio			0.005[a]
≥1	26	82	
<1	48	66	
Diffuse disease			0.503[a]
Yes	15	37	
No	59	111	

Table II. Continued.

Parameter	Benign (n=74)	Malignant (n=148)	P-value
Micro-calcification			<0.001[a]
Yes	8	79	
No	66	69	
D. ES.			
Elasticity ratio	1.37±0.39	1.86±0.91	<0.001[b]
Area ratio (%)	35.09±21.63	50.19±25.25	<0.001[b]
E. CD US.			
Blood flow extent			<0.001[b]
Low: A little 'dot-like' blood flow detected	23	125	
Moderate: Area of vascularity detected occupied about one-half of the nodules	34	11	
High: Area of vascularity was demonstrated in more than one-half of nodules	17	11	
Central vessels			<0.001[b]
Yes	46	30	
No	28	118	
Surrounding vascular ring			<0.001[b]
Yes	46	7	
No	28	141	

Patterns in CE US: Pattern I, heterogeneous hypoenhancement; Pattern II, homogeneous isoenhancement; Pattern III, homogeneous enhance ment with ring-like surrounding vascularity, mixed island-like enhancement or no perfusion. [a]Calculated with the χ^2 test. [b]Calculated with the independent sample t-test. US, ultrasonography; CD US, color Doppler ultrasonography; ES, elastosonography; CE US, contrast-enhanced ultrasonography; A/T ratio, ratio of anteroposterior to transverse dimension.

Table III. Parameters selected for use in developing the decision tree after multivariate logistic analysis.

Parameters	P-value	Odds ratio	95% confidence interval
Peak-phase patterns on contrast enhanced ultrasonography	<0.01	245.52	23.72-2541.63
Area ratio on ES	0.03	3.26	1.10-9.71
Extent of blood flow	<0.01	0.144	0.02-1.12
Micro-calcification on conventional gray-scale ultrasonography	0.015	4.73	1.35-16.61

ES, elastosonography.

Results

The demographic data and features of the US images obtained for 289 nodules are shown in Table I.

For ES as a continuous variable, the cutoff point obtained using the ROC curve was 46.5% for area ratio and 1.215 for elasticity index. According to these values, area ratio was divided into two groups: ≥46.5% (55 benign and 93 malignant) and <46.5% (56 benign and 18 malignant). Elasticity index was categorized as follows: ≥1.215 (33 benign and 115 malignant) and <1.215 (38 benign and 36 malignant), which was used for logistic analysis (Table II).

After univariate logistic analysis, as indicated in Table II, the P-values for sex, number of nodules and diffuse disease were >0.1 and so these factors were excluded from further analysis. The following parameters, with P<0.001, were employed for multivariate logistic analysis: Diameter, echogenicity, ring-halo sign, margin, shape, A/T ratio, micro-calcification, extent of blood flow, central vessels, surrounding vascularity, area ratio, elasticity index and enhancement patterns during the early, peak and late phases. The results of the multivariate logistic analysis demonstrated the significant effects of four parameters (Table III), which were selected for use in developing the DT (Fig. 5).

In the DT, peak-phase patterns on CEUS were evaluated as the first step, followed by area ratio on ES. CDUS and micro-calcification on conventional gray-scale US were then used for further diagnosis (Fig. 5). When the DT was

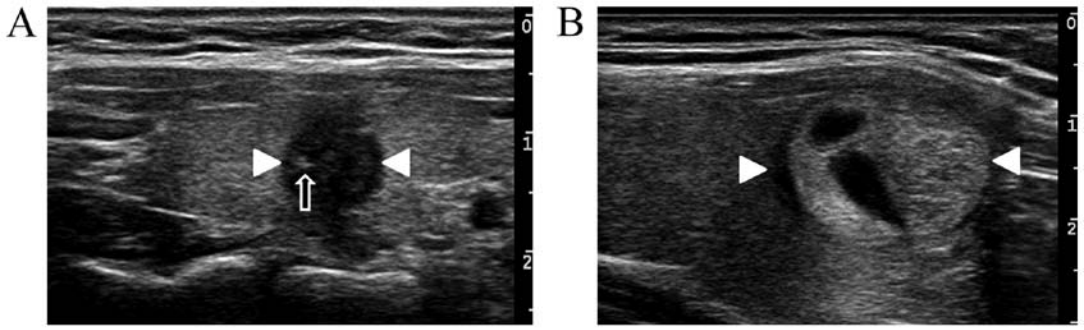

Figure 2. Conventional gray-scale ultrasonography. (A) One malignant nodule (white arrowheads) of a 38-year-old woman with hypoechogenicity and an unclear margin, irregular shape, micro-calcification (black arrow) and an A/T >1, and without a halo ring or diffuse changes in the surrounding areas. (B) One benign nodule (white arrowheads) in a 48-year-old woman with isoechogenecity mixed with anechogenecity, clear margin, regular shape, A/T <1, a halo ring, and no micro-calcification or diffuse changes in the surrounding areas. A/T, anteroposterior to transverse dimension.

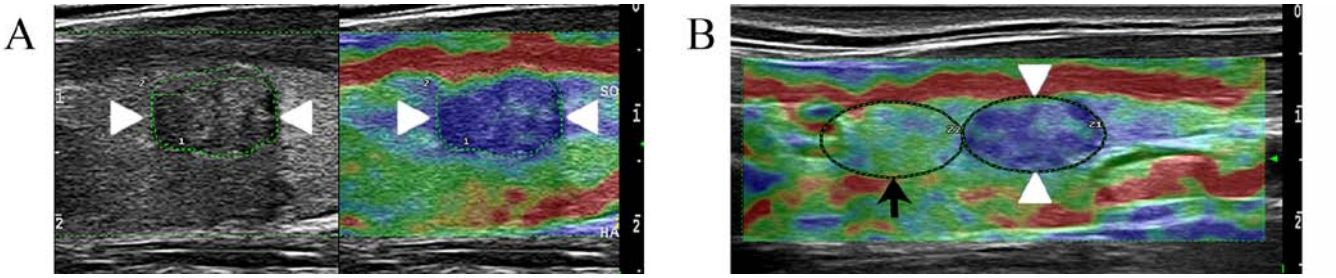

Figure 3. Elastosonographic images in a thyroid nodule of a 51-year-old woman. (A) The area ratio was calculated by dividing the hardest region of the nodule (shown in blue) by the total nodule area. (B) The elasticity index was calculated by dividing the hardness of the nodule (white arrowheads) by the hardness of an equivalently sized nearby area (black arrows).

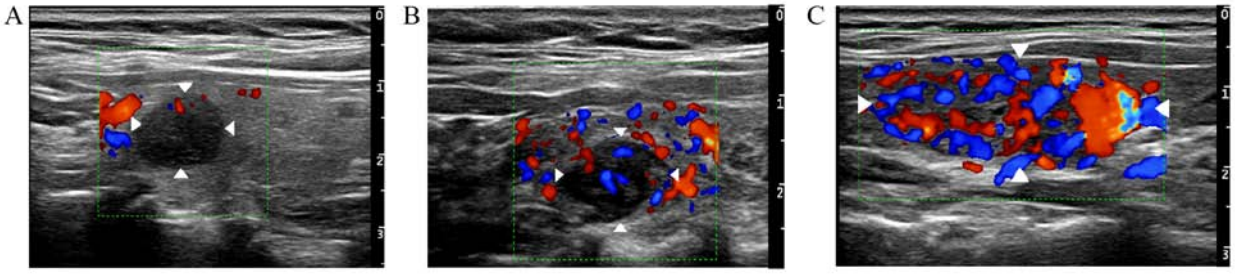

Figure 4. Extent of blood flow in thyroid nodules as revealed by color Doppler ultrasonography. (A) Low, only 'dot-like' blood flow was detected in a thyroid nodule of a 35-year-old woman. (B) Moderate, area of vascularity detected in a thyroid nodule of a 38-year-old man occupied about half of the nodule. (C) High, area of vascularity occupied more than half the nodule in a 47-year-old woman. White arrowheads indicate thyroid nodules.

retrospectively applied to the pathology or cytology results of the 99 test nodules, it displayed a sensitivity of 98.6% (95% CI: 91.6-99.9%), specificity of 80.1% (95% CI: 60.0-92.7%), positive predictive value of 93.5% (95% CI: 84.8-97.6%) and negative predictive value of 95.5% (95% CI: 75.1-99.8%) (Fig. 6).

Discussion

US techniques offer much useful information for differentiating benign from malignant thyroid nodules (19,20). However, in some cases the information obtained from various US techniques can be contradictory and these various pieces of information need to be integrated efficiently. Although the combined application of multiple US techniques has been reported previously (21,22), the current study established a novel algorithm to integrate four different techniques to improve the differential diagnosis of thyroid nodules.

CEUS patterns have been shown to be useful in differentiating benign from malignant thyroid lesions (23-25). Ring enhancement was mostly considered a predictive sign of benignity, whereas heterogeneous hypoenhancement was predictive of malignant lesions (24,25). The results of the present study were consistent with these findings, and malignant nodules were also detectable by homogeneous isoenhancement. Some inflammatory nodules presented hypoenhancement similar to that of malignant nodules. Thus, the CEUS patterns of thyroid nodules with overlapping characteristics between benign and malignancy appear to be relatively more complex than those of liver lesions. Additional parameters will need to be considered for the development of a thorough predictive model.

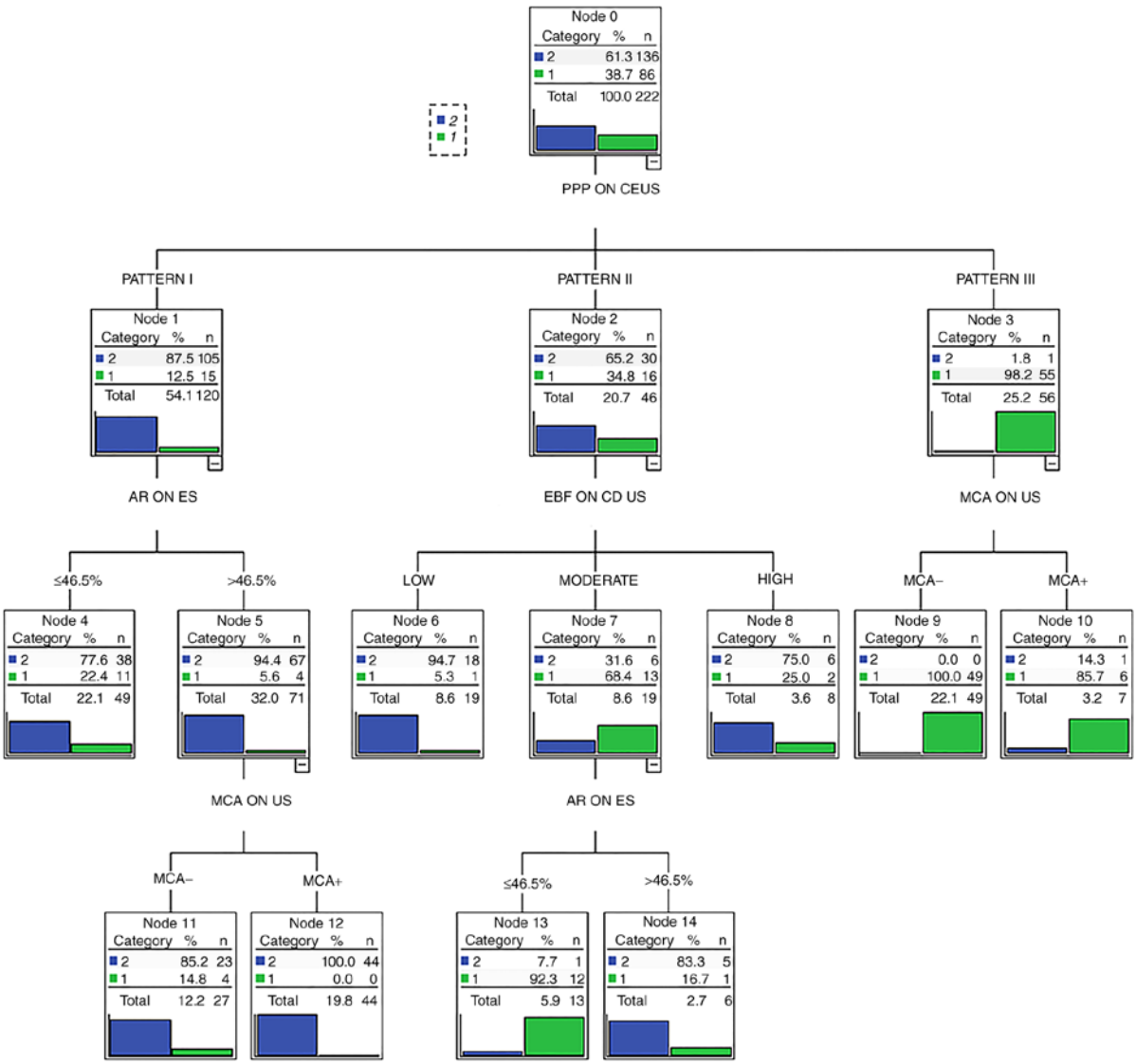

Figure 5. Decision tree obtained using parameters from gray-scale US, color Doppler US, ES and CEUS. Pattern I, heterogeneous hypoenhancement on CEUS. Pattern II, homogeneous isoenhancement on CEUS. Pattern III, homogeneous enhancement with ring-like surrounding vascularity, mixed island-like enhancement, or no perfusion on CEUS. PPP, peak phase pattern; AR, area ratio; CEUS, contrast-enhanced ultrasonography; ES, elastosonography; EBF, extent of blood flow; US, ultrasonography; MCA, micro-calcification.

Previously developed algorithms for diagnosing thyroid nodules have integrated ES analysis (26,27). In a study of 141 nodules, most of the benign nodules scored in the range 2-3, while malignant nodules scored ~5 (26). Giusti *et al* (28) reported that the information added by CEUS is less sensitive than that provided by US and ES. However, the results of that study may have been influenced by the relatively small number of malignant lesions. In the current study, area ratio was found to be a useful factor in logistic multivariate regression. In the DT algorithm, nodules with homogenous isoenhancement, moderate blood flow and ES area ratio >46.5% were classified as malignant.

On conventional gray-scale US, spongiform and cystic features seem to provide sufficient information to confidently rule out cancer (29) and calcification is regarded as a significant indicator of malignancy (30). In the current study, on conventional gray-scale US only 'micro-calcification' was included in the final algorithm, while shape, margin and echogenicity

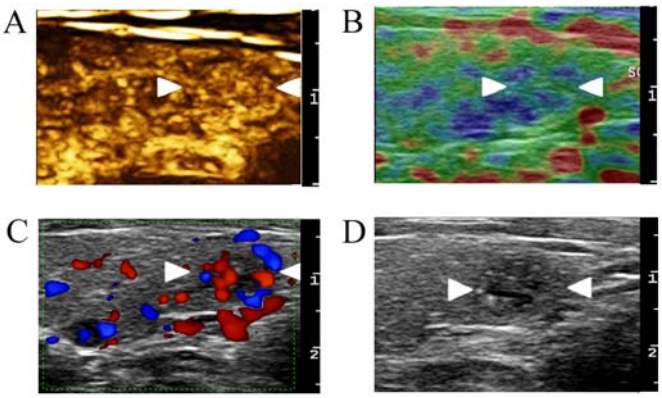

Figure 6. A case of thyroid papillary carcinoma with a diameter of 0.7 mm in a 55-year-old man, correctly identified as malignant by the decision tree algorithm. (A) Contrast enhanced sonography revealed homogeneous enhancement within the nodule (Pattern II). (B) The area ratio as determined by electrosonography was 67.1%. (C) The nodule showed a moderate level of blood flow. (D) On conventional gray-scale ultrasonography, the nodule appeared hypoechoic and ill-defined. White arrows indicate the nodule.

were excluded. This may be explained in several ways. First, there could be a parallel statistical influence of a given parameter on multiple techniques. For example, the US 'halo-ring' may also be related to ring enhancement on CEUS. Second, in this retrospective study, some patients underwent CEUS only after uncovering an atypical appearance using conventional gray-scale US. Thus, the data from conventional gray-scale US were not necessarily the most useful. Finally, 52 of 222 nodules were depicted with diffuse changes to the thyroid gland, influencing appearance and the diagnostic accuracy of conventional gray-scale US.

As some nodules appear to show atypical features on conventional gray-scale US, especially in the background of an inflamed thyroid, it has always been a challenge to confirm diagnosis using conventional gray-scale US. In the current study, 18 of these 24 inflammatory nodules were depicted with hypoenhancement with a low to medium level of blood flow, a similar appearance to that observed in malignant nodules. However, most of these nodules (15 of 18) had an area ratio <46.5% on ES, which meant there was low stiffness within these nodules, implying benignity. These findings imply that a DT algorithm combining four US techniques may supply a new method for the diagnosis of inflammatory nodules.

The current preliminary study has several limitations. First, as this is a retrospective study, the patients were examined as part of routine work and their images were reviewed. Therefore, the number of nodules was limited as cases lacking pathological or cytological results were excluded. Second, nodules identified as 'typical' by US were not further examined using CEUS and thus were not included in this study, perhaps influencing the results of the DT. Finally, in testing 99 nodules with the final DT, five nodules were falsely identified as malignant, including four with diameter <10 mm. One false benign nodule <10 mm in diameter presented isoenhancement on CEUS. The results of this study therefore need to be verified in more patients and future analysis of typical and very small nodules would be beneficial.

In conclusion, combining the parameters available on CEUS, conventional gray-scale US and ES with CDUS in this preliminary study allowed establishment of a DT algorithm that could be helpful for the differential diagnosis of thyroid nodules. Use of this algorithm could allow clinicians to integrate information from multiple US techniques and clarify an otherwise ambiguous diagnosis, leading to improved treatment options and prognosis.

Acknowledgements

Not applicable.

Funding

This study was funded by the financial support of the National Natural Science Fund (grant no. 81671691).

Availability of data and materials

The datasets used and/or analyzed during the current study are available from the corresponding author on reasonable request.

Authors' contributions

WL was responsible for the study design, data analysis, data acquisition and manuscript preparation. YZ was responsible for study design, data analysis and manuscript preparation. JY was responsible for data analysis and manuscript editing. XY was responsible for literature research and data acquisition. LP was responsible for acquisition of data, data analysis and manuscript editing. LD was responsible for statistical analysis and the layout and correction of the parts of the article. PZ was responsible for data analysis and figure adjustment. LL was responsible for manuscript editing and data acquisition. XZ was responsible for the study design and data analysis, is the guarantor of the integrity of the entire study and gave manuscript final version approval.

Ethics approval and consent to participate

This study was approved by The Ethics Committee of the First Affiliated Hospital of the Fourth Military Medical University and the requirement for patients to provide written informed consent was waived by the hospital because this was a retrospective study.

Patient consent for publication

Not applicable.

Competing interests

The authors declare that they have no competing interests.

References

1. Moon WJ, Baek JH, Jung SL, Moon WJ, Baek JH, Jung SL, Kim DW, Kim EK, Kim JY, Kwak JY, *et al*: Ultrasonography and the ultrasound-based management of thyroid nodules: Consensus statement and recommendations. Korean J Radiol 12: 1-14, 2011.
2. Wang Y and Wang W: Increasing incidence of thyroid cancer in Shanghai. China, 1983-2007. Asia Pac J Public Health 27: NP223-NP229, 2015.
3. Kitahara CM and Sosa JA: The changing incidence of thyroid cancer. Nat Rev Endocrinol 12: 646-653, 2016.
4. Acar T, Ozbek SS and Acar S: Incidentally discovered thyroid nodules: Frequency in an adult population during Doppler ultrasonographic evaluation of cervical vessels. Endocrine 45: 73-78, 2014.
5. Paschke R, Hegedüs L, Alexander E, Valcavi R, Papini E and Gharib H: Thyroid nodule guidelines: Agreement, disagreement and need for future research. Nat Rev Endocrinol 7: 354-361, 2011.
6. Hoang JK, Riofrio A, Bashir MR, Kranz PG and Eastwood JD: High variability in radiologists' reporting practices for incidental thyroid nodules detected on CT and MRI. AJNR Am J Neuroradiol 35: 1190-1194, 2014.
7. Lim HK, Park ST, Ha H and Choi SY: Thyroid nodules detected by contrast-enhanced magnetic resonance angiography: Prevalence and clinical significance. PLoS One 11: e0149811, 2016.
8. Kim TH, Ji YB, Song CM, Kim JY, Choi YY, Park JS and Tae K: SUVmax of 18F-FDG PET/CT in the differential diagnosis of benign and malignant thyroid nodules according to tumor volume. World J Surg Oncol 13: 217, 2015.
9. Richmond B, Statler K, Judhan R, Mangano W and Thompson S: Sonographic appearance is useful in predicting the extent of initial operative therapy for thyroid nodules classified as 'suspicious for malignancy'. Am Surg 82: 692-697, 2016.
10. Palaniappan MK, Aiyappan SK and Ranga U: Role of gray scale, color Doppler and spectral Doppler in differentiation between malignant and benign thyroid nodules. J Clin Diagn Res 10: TC01-TC06, 2016.

11. Zhang Y, Luo YK, Tang J, Li M, Wang ZL and Wen Q: Clinical value of ultrasonography in diagnosing diffuse thyroid diseases accompanied with suspicious nodules. Zhongguo Yi Xue Ke Xue Yuan Xue Bao 37: 290-293, 2015.
12. Chen HY, Liu WY, Zhu H, Jiang DW, Wang DH, Chen Y, Li W and Pan G: Diagnostic value of contrast-enhanced ultrasound in papillary thyroid microcarcinoma. Exp Ther Med 11: 1555-1562, 2016.
13. He Y, Wang XY, Hu Q, Chen XX, Ling B and Wei HM: Value of Contrast-enhanced ultrasound and acoustic radiation force impulse imaging for the differential diagnosis of benign and malignant thyroid nodules. Front Pharmacol 27: 1363, 2018.
14. Zhan J and Ding H: Application of contrast-enhanced ultrasound for evaluation of thyroid nodules. Ultrasonography 37: 288-297, 2018.
15. Magri F, Chytiris S and Chiovato L: The role of elastography in thyroid ultrasonography. Curr Opin Endocrinol Diabetes Obes 23: 416-422, 2016.
16. Cantisani V, D'Andrea V, Biancari F, Medvedyeva O, Di Segni M, Olive M, Patrizi G, Redler A, De Antoni EE, Masciangelo R, *et al*: Prospective evaluation of multiparametric ultrasound and quantitative elastosonography in the differential diagnosis of benign and malignant thyroid nodules: Preliminary experience. Eur J Radiol 81: 2678-2683, 2012.
17. Zhang Y, Zhou P, Tian SM, Zhao YF, Li JL and Li L: Usefulness of combined use of contrast-enhanced ultrasound and TI-RADS classification for the differentiation of benign from malignant lesions of thyroid nodules. Eur Radiol 4: 1527-1536, 2017.
18. Sui X, Liu HJ, Jia HL and Fang QM: Contrast-enhanced ultrasound and real-time elastography in the differential diagnosis of malignant and benign thyroid nodules. Exp Ther Med 12: 783-791, 2016.
19. Ferrari FS, Megliola A, Scorzelli A, Guarino E and Pacini F: Ultrasound examination using contrast agent and elastosonography in the evaluation of single thyroid nodules: Preliminary results. J Ultrasound 11: 47-54, 2008.
20. Zhang YZ, Xu T, Gong HY, Li CY, Ye XH, Lin HJ, Shen MP, Yang DT and Wu XH: Application of high-resolution ultrasound, real-time elastography, and contrast-enhanced ultrasound in differentiating solid thyroid nodules. Medicine (Baltimore) 95: e5329, 2016.
21. Reginelli A, Urraro F, di Grezia G, Napolitano G, Maggialetti N, Cappabianca S, Brunese L and Squillaci E: Conventional ultrasound integrated with elastosonography and B-flow imaging in the diagnosis of thyroid nodular lesions. Int J Surg 12 (Suppl 1): S117-S122, 2014.
22. Zhao RN, Zhang B, Yang X, Jiang YX, Lai XJ and Zhang XY: Logistic regression analysis of contrast-enhanced ultrasound and conventional ultrasound characteristics of sub-centimeter thyroid nodules. Ultrasound Med Biol 41: 3102-3108, 2015.
23. Argalia G, De Bernardis S, Mariani D, Abbattista T, Taccaliti A, Ricciardelli L, Faragona S, Gusella PM and Giuseppetti GM: Ultrasonographic contrast agent: Evaluation of time-intensity curves in the characterisation of solitary thyroid nodules. Radiol Med 103: 407-413, 2002 (In English, Italian).
24. Zhang Y, Luo YK, Zhang MB, Li J, Li J and Tang J: Diagnostic accuracy of contrast-enhanced ultrasound enhancement patterns for thyroid nodules. Med Sci Monit 22: 4755-4764, 2016.
25. Jiang J, Shang X, Zhang H, Ma W, Xu Y, Zhou Q, Gao Y, Yu S and Qi Y: Correlation between maximum intensity and microvessel density for differentiation of malignant from benign thyroid nodules on contrast-enhanced sonography. J Ultrasound Med 33: 1257-1263, 2014.
26. Tatar IG, Kurt A, Yilmaz KB, Doğan M, Hekimoglu B and Hucumenoglu S: The role of elastosonography, gray-scale and colour flow Doppler sonography in prediction of malignancy in thyroid nodules. Radiol Onco 48: 348-353, 2014.
27. Li F, Zhang J, Wang Y and Liu L: Clinical value of elasticity imaging and contrast-enhanced ultrasound in the diagnosis of papillary thyroid microcarcinoma. Oncol Lett 10: 1371-1377, 2015.
28. Giusti M, Campomenosi C, Gay S, Massa B, Silvestri E, Monti E and Turtulici G: The use of semi-quantitative ultrasound elastosonography in combination with conventional ultrasonography and contrast-enhanced ultrasonography in the assessment of malignancy risk of thyroid nodules with indeterminate cytology. Thyroid Res 7: 9, 2014.
29. Brito JP, Gionfriddo MR, Nofa AA, Boehmer KR, Leppin AL, Reading C, Callstrom M, Elraiyah TA, Prokop LJ, Stan MN, *et al*: The accuracy of thyroid nodule ultrasound to predict thyroid cancer: Systemic review and meta-analysis. J Clin Endocrinol Metab 99: 1253-1263, 2014.
30. Li JW, Chang C, Chen M, Zeng W, Gao Y, Zhou SC, Wang F, Hu N and Chen YL: Is ultrasonography more sensitive than computed tomography for identifying calcifications in thyroid nodules? J Ultrasound Med 35: 2183-2190, 2016.